Laboratory Report 3
Photometry With An Infrared Camera

Kirsten Howley [1]
Group 2
October 16, 2001

1. BACKGROUND & MOTIVATION

Since astronomy is essentially governed by our ability to obtain and interpret images, it is necessary to understand the tools and techniques used in observing and analyzing astronomical objects. It can be anticipated that any equipment used for observation will posses certain limitations, thus imposing errors on data acquired from it. Such errors are caused by both defects in the detector and by extra photons collected from the overlying sky, thermal fluctuations and Poisson noise. Our goal in this lab is calculate these errors for images of stars with known magnitudes in order to determine the necessary exposure time to acquire a given signal-to-noise ratio.

2. EQUIPMENT & METHOD

The first part of the experiment involved determining how to operate the telescope and locate images in the sky. The Leuschner 30-inch telescope operates on celestial coordinates. For this reason, it was important to understand the conversion between terrestrial coordinates(azimuth, elevation) and celestial coordinates(right ascension, declination). Azimuth corresponds to the location relative to the north pole; more specifically, azimuth instructs the observers to turn to the north, east, south, west, or any combination between. Elevation indicates the inclination of the object relative to the horizon.

Celestial coordinates correspond to points and the celestial sphere, whose north pole, south pole, and equator corresponding to those of the Earth. It is more convenient system to use because, unlike terrestrial coordinates, the position of an object has fixed coordinates associated with it, so that the only thing changing is the position of the observer relative to the sphere. Right ascension is the 'longitude' of the object on the celestial sphere. The position of a star relative to the meridian can be expressed using local sidereal time and hour angle. The hour angle measures how far east or west an object is relative to the meridian. Local sidereal time is like the hand that measures the time on a clock; a local sidereal day is 23 hours, 56 minutes and 4 seconds long and is related to hour angle and right ascension by:

$$Hour\ Angle = Local\ Sidereal\ Time - Right\ Ascension$$

Figure 1 demonstrates the conversion between local sidereal time and elevation for the star HD 3029.

[1] E-mail: kirsten@ugastro.berkeley.edu

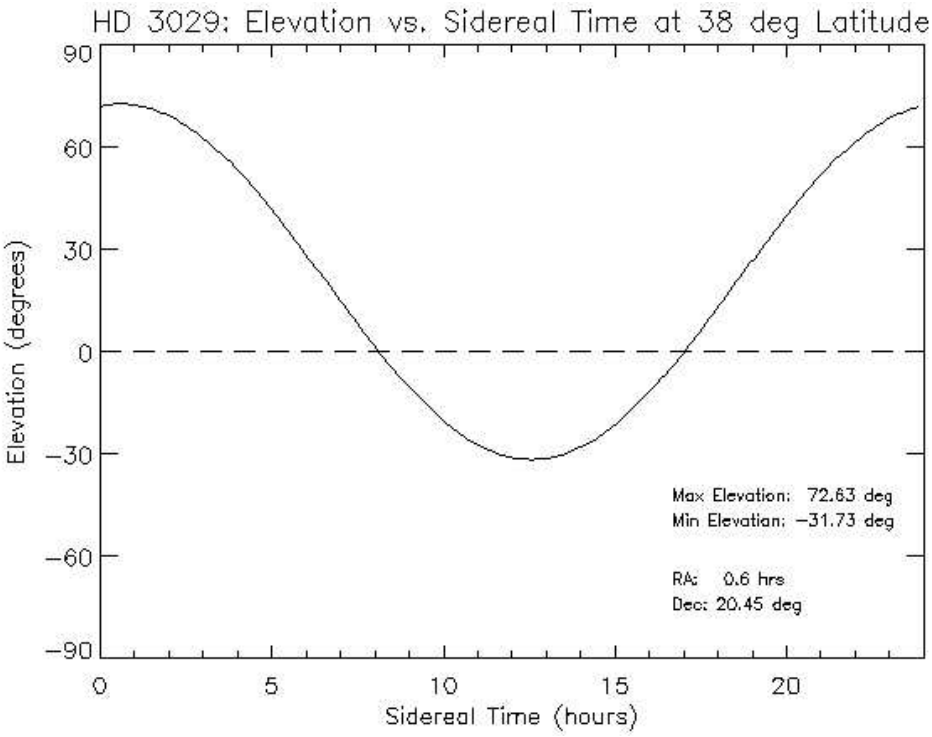

Fig. 1.— Elevation

When converting coordinate systems, it is important to include the position of the observer in respect to the celestial equator, since this directly affects the angle at which the celestial sphere is viewed. Once the observers position, and the star's celestial coordinates are known, celestial coordinates can be transformed into terrestrial coordinates. The following will convert latitude (lat), declination (dec), and hour angle (ha) into elevation (el) and azimuth (az):

$$el = sin^{-1}\left(sin(lat)sin(dec) - cos(lat)cos(dec)cos(ha)\right)$$

$$az = cos^{-1}\left(\frac{sin(dec) - sin(lat)sin(el)}{cos(lat)cos(el)}\right)$$

Taking images from the Leuschner telescope and infrared camera involved a remote login to the system 128.32.197. Once in the system, the dome needed to be opened and positioned to look out the slit, a filter need to be selected (the K filter and aluminum plug were used for this lab), the flip mirror had to be opened, and the telescope had to be focused and pointed at the desired location. Since the Leuschner telescope operates on celestial coordinates, one needed to verify that the desired object was presently within viewing range (above the horizon) before imaging an object. Images were taken with selected exposure times using the *qimage* command. Files were exported from the remote system into the local system using *sftp*. Detailed log sheets were kept for images collected from the telescope, and can be accessed at enielsen/lab03/l3.logsheets/.

3. DATA COLLECTION & ANALYSIS

One of the limitations of the detector is the number of photons it is able to collect during an imaging sequence. The detector can be saturated by both stars of various magnitudes and by the general sky background. For this reason, the saturation level of the detector was first determined. This was done by collecting images with increasing exposures times and plotting the corresponding average number of counts per pixel. Since the temperature of the device affects its sensitivity, saturation levels were determined during both the afternoon and evening. The results are plotted in Figure 1. Saturation during daylight exposure occurred at 6.6 seconds, or 20,000 counts; saturation for evening exposure occurred at 33 seconds, or 22,000 counts. This variance in count saturation is due to the temperature sensitivity of the detector; at higher temperatures, the detector saturates with fewer counts than at lower temperatures.

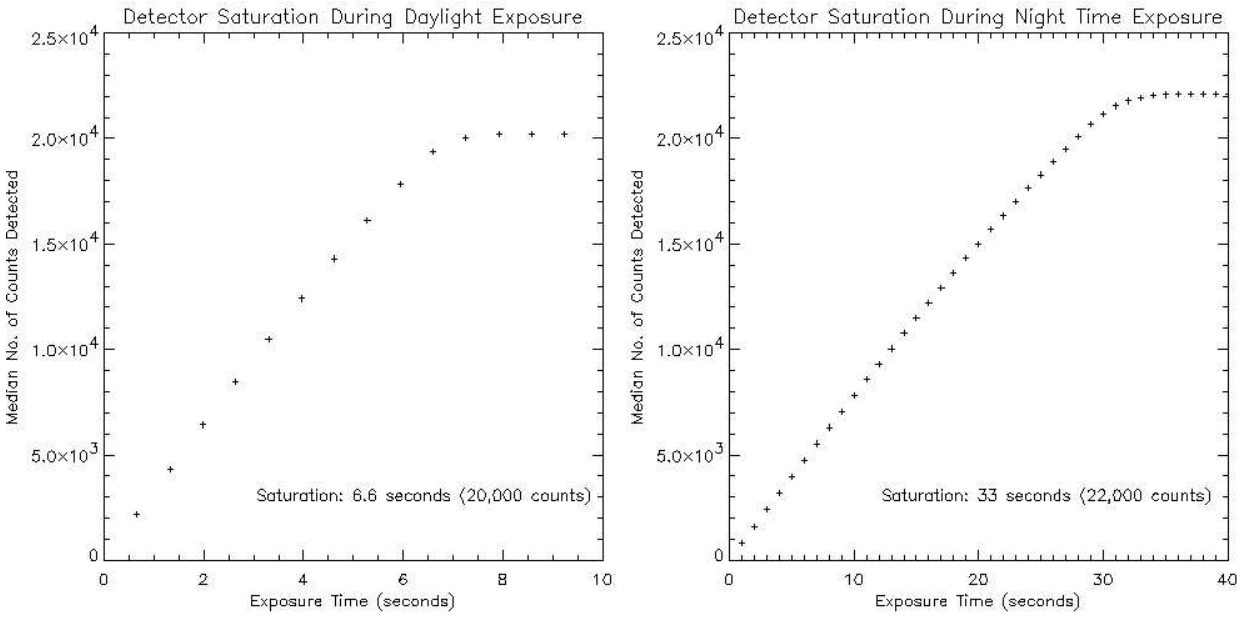

Fig. 2.— Saturation of the detector during both daylight and evening exposure. To be sure not to saturate the detector during imaging, exposure times much less than 33 seconds were selected. Note that the detector saturated at a lower count rate during the day, when the detector was warmer.

Another important aspect of the equipment sensitivity that needed to be considered was the dark counts it collected during exposure. Dark counts are photons recorded by the detector when no light is purposefully being collected. Since nearly everything on Earth emits in the infrared spectrum, there is a constant flux of photons from surrounding sources. To determine how many photons were due to sources other than the sky, images were taken with an aluminum plug filter with increasing exposure times. Due to the fact that the number of counts recorded by the detector is temperature related, each time stellar images were taken, a set of dark images were also taken

in attempt to approximate the corresponding dark current at that time.

Unfortunately, dark frames have noise associated with them, and thus contribute error. We can reduce the noise by increasing the number of averaged dark images. The number of images needed, N, can be calculated by treating each pixel in a single dark image as a mean and computing the standard deviation of those individual means. If we want to ensure that our dark frame increases the noise by no more than 10%:

$$10\% = \left(\frac{1}{\sqrt{N}}\right)\frac{SDOM}{Mean\sqrt{\#\,of\,pixels}}$$

or,

$$N = \left(\frac{1}{0.1^2}\right)\frac{SDOM^2}{Mean^2(\#\,of\,pixels)}$$

Using a 4 second dark image exposure, it was determined that one image was more than sufficient in producing a fractional error of less than 10%. The image used had a standard deviation (SDOM) of 165 counts and a mean of 493 counts. Since each pixel corresponds to a sample, or a mean, the 65,536 (256 x 256) pixels yielded a fractional error of 0.1%:

$$.01\% = \frac{1}{\sqrt{1\ image}}\frac{165\ counts}{493\ counts\sqrt{256^2\ pixels}}$$

Because our telescope operates in a similar way to the CCD camera, there is also a conversion factor between counts and photoelectrons, $\left(\frac{gain}{capacitance}\right)$, as well as a readout noise, $/sigma_{read\,out\,noise}$, associated with it. From Lab 2, the variance and the signal can be related using this conversion factor and readout noise by[2]:

$$s^2 = signal\frac{gain}{capaciatance} + \sigma^2_{read\,out\,noise}\frac{gain^2}{capaciatance^2} \tag{1}$$

Duplicate images with increasing exposure times were collected of the dome (taken with the K filter), along with corresponding darks (taken with the aluminum plug). To construct an array of values for s^2, two images of the dome (with the same exposure times) were subtracted, and the variance was calculated. The values used for the signal were obtained by subtracting a dark image from an illuminated image in order to isolate the signal. Using the process of *Least Squares Fitting*, a best fit line was constructed to determine the slope and y-intercept of the data points. Figure 3 displays the results.

From Equation 1, the readout noise can be calculated from the y-intercept and the slope of the extrapolated line in Figure 3. The readout noise, in photoelectrons is:

$$intercept = \sigma^2_{read\,out\,noise}\frac{gain^2}{capaciatance^2}$$

[2]Lab 2, Equation 6

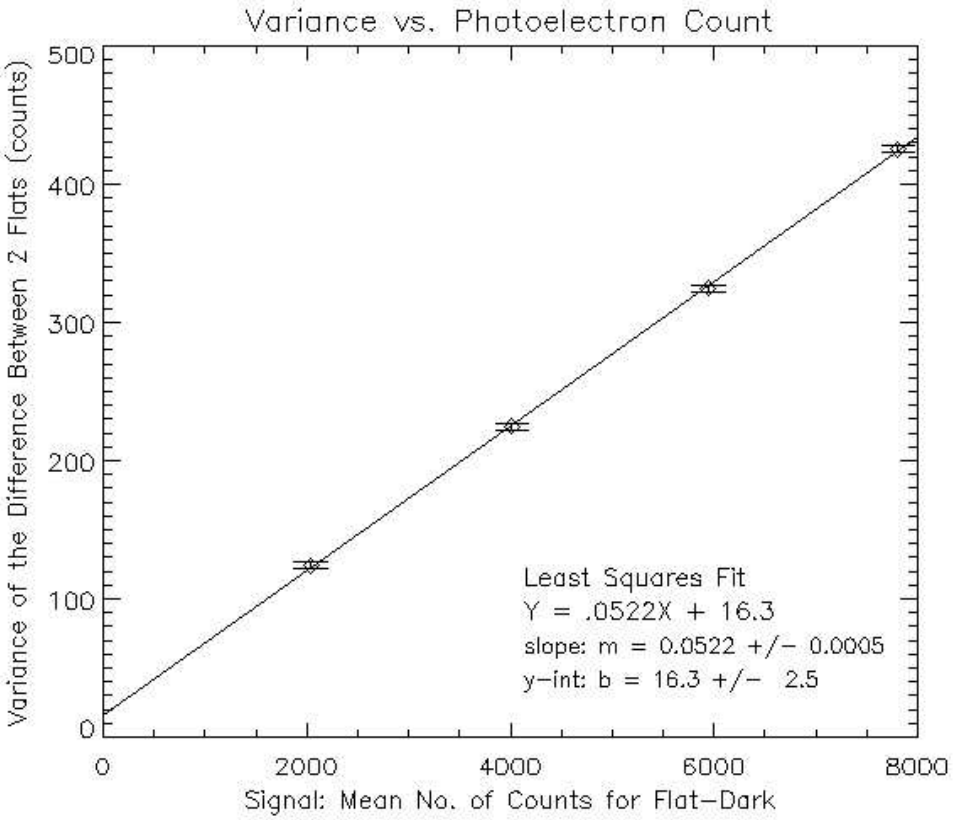

Fig. 3.— Variance vs. Photoelectron count. Data acquired of evenly illuminated image with increasing exposure times. The technique of least squares was used to fit a straight line to the points in order to determine the gain and readout noise of the detector.

$$\sigma_{readout\,noise} = \frac{\sqrt{intercept}}{slope} \approx 80\,photoelectrons \tag{2}$$

And the $\frac{gain}{capacitance}$, which is the conversion factor between counts and photoelectrons, is:

$$\frac{gain}{capacitance} = slope = .0522 \pm .0005\,counts/photoelectron$$

The errors in these measurements are calculated using the propagation of errors techniques from Lab 2, and are also included in Figure 3[3].

In addition to the dark current, the varying sensitivity on a pixel to pixel basis of the detector must also be considered. A map of this variation is called a flatfield. The flatfield can be constructed by evenly illuminating the detector to determine how each pixel responds to a constant flux of

[3]Original equations obtained from Taylor, John R.

photons. We are able to closely approximate even illumination by imaging the sky at twilight or dusk. We assume that during this time the sky brightness, B_i, is uniform, and therefore a constant. Using a twilight image, $z_i(x, y)$, and the mean dark current image, $c(x, y)$, the constant sky brightness for each twilight image can be estimated:

$$B_i = median[z_i(x, y) - c(x, y)]$$

The variations in the fully illuminated image are a function of the relative gain per pixel, the sky brightness, and the constant dark signal and arbitrary offset:

$$z_i(x, y) = f(x, y)B_i + c(x, y) \tag{3}$$

Using Equation 3, and the assumption that the relative pixel gain is 1, the flatfield image was constructed by:

$$g(x, y) = \left\langle \frac{z_i(x, y) - c(x, y)}{B_i} \right\rangle$$

Figure 4 displays the calculated flatfield. The image on the left is displayed within two standard deviations. The image on the right is a three dimensional plot showing the relative gain per pixel. The sharp inverted spikes are most likely due to bad pixels in the detector. A more thorough analysis of the flatfield would involve weighting these pixels, thus creating a weighted pixel map, and excluding values obtained from their particular locations in future stellar calculations.

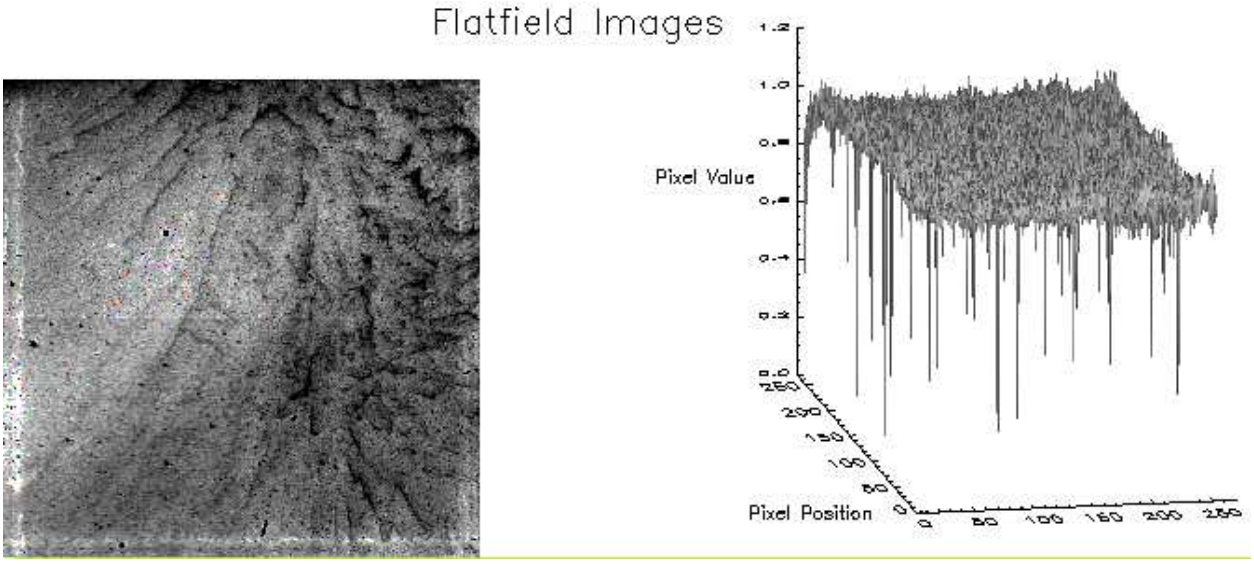

Fig. 4.— The left image is a tvscl view of the flatfield scaled within two standard deviations. The right image is a three dimensional plot showing the relative gain per pixel.

Of course, using the flatfield increases our error. We can decrease our error by increasing the amount of data collected. If our data is converted from counts to photoelectrons, we can use

Poisson statistics to express the errors in our data. From propagation of errors, the error in our flatfield is given by the sum of the variances:

$$s^2_{flat} = s^2_{sky} + s^2_{dark} + 2\sigma^2_{readout\,noise} \tag{4}$$

The fractional error is given by:

$$\frac{s^2_{flat}}{\langle flat \rangle} = \frac{s^2_{sky} + s^2_{dark} + 2\sigma^2_{readout\,noise}}{\langle flat \rangle} \tag{5}$$

The readout noise is included twice because there is a readout noise associated with both the sky images and the dark images. It was added into Equations 4 & 5 for clarity. It is, in fact, part of the error in the dark and sky images:

$$s^2_{dark} = \frac{\langle dark \rangle}{N} + \sigma^2_{readout\,noise}$$

This equation can be used to determine the error in either a dark or sky image, once they have been converted into photoelectrons. The value for $\sigma_{readout\,noise}$ is given in Equation 2. Since in our original calculation of the flatfield, we divided by a constant sky brightness, we must account for this constant in the calculation of our error. That is if $z = \frac{x}{A}$, where A is a constant, then the errors are related by:

$$\sigma^2_x = \frac{1}{N-1}\sum_{i=0}^{N}(x - \bar{x})^2$$

$$\sigma^2_z = \frac{1}{N-1}\sum_{i=0}^{N}\left(\frac{x}{A} - \frac{\bar{x}}{A}\right)^2$$

$$\sigma_z = \frac{1}{A}\sigma_x$$

Using 10 dark and sky images, the fractional error in the flat was computed and found to be:

$$\frac{\sigma_{flat}}{\langle flat \rangle} = .0008\%$$

Much less than 1% of our flatfield image!

Flatfields and Dark Images are both used to reduce the noise in our images and, thus, extract the signal from our star. The signal from a star is usually spread out over several pixels. A circular aperture is used to isolate the light solely from our star. A radius of 3.0σ encompasses 99% of the light, determined from the normal distribution function. If $P(x, y)$ is the probability of a measurement occurring between (x_1, x_2) and (y_1, y_2), then the probability of this measurement is given by[4]:

[4]Taylor, John R.

$$P(x,y) = \frac{\int_{y_1}^{y_2}\int_{x_{-1}}^{x_2} e^{\frac{1}{2}\frac{x^2+y^2}{\sigma^2}}\,dx\,dy}{\int_{-\infty}^{\infty}\int_{-\infty}^{\infty} e^{\frac{-1}{2}\frac{x^2+y^2}{\sigma^2}}\,dx\,dy}$$

Using the symmetry of our two dimensional image, which has an area of $\pi(n\sigma)^2$, we can convert from Cartesian to spherical coordinates to compute the probability function:

$$r^2 = x^2 + y^2$$

$$dx\,dy = r\,dr\,d\theta$$

And our probability function becomes:

$$P(r,\theta) = \frac{\int_0^{2\pi}\int_0^{n\sigma} e^{\frac{-1}{2}\frac{r^2}{\sigma^2}} r\,dr\,d\theta}{\int_0^{2\pi}\int_0^{\infty} e^{\frac{-1}{2}\frac{r^2}{\sigma^2}} r\,dr\,d\theta} \tag{6}$$

Using substitution of variables and integrating yields the following results for different values of n,

$$n = 1,\ P(\sigma) = 0.39 \qquad n = 2,\ P(2\sigma) = 0.87 \qquad n = 3,\ P(3\sigma) = 0.99$$

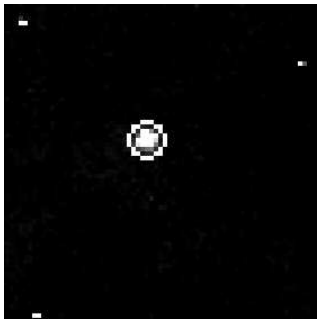

Fig. 5.— Area inside the circle encompasses 99% of the light from the stellar image located in the center. These apertures were used to extract the signal from the star.

A program was constructed to locate the pixel with the largest number of counts within a ten pixel radius of a selected point. A circle aperture was then used to isolate the star, as shown in Figure 5. Dark current was subtracted from the image, and the flatfield was applied in an attempt to reduce the noise. However, upon inspection, there were still counts present in the neighboring pixels. Since sky brightness is not entirely uniform, the sky level needed to be determined in the vicinity of the star. This was done by constructing an annular ring with an inner radius of 6σ and an outer radius of 8σ. These dimensions were chosen to ensure that the sample taken would include the sky brightness, but not any counts from the star. It can be shown from Equation 6 that 6σ includes very close to 100% of the starlight. Figure 6 displays an example of an annular ring used.

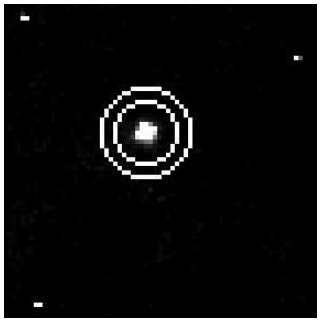

Fig. 6.— The signal inside the annulus determined the local sky brightness level. This aperture was used to obtain a better estimate of sky level.

It can be anticipated that by removing this background noise, as you sum the signal in increasing radii, eventually the signal will fail to increase with increasing radius. This is because the starlight is pretty much contained within the first few sigma, and the surrounding background has an average value of zero counts. Figure 7 shows a plot of the pixel sum as a function of pixel radius for the star HD 203856. Notice how the values steadily increase and then plateau. The pixels adjacent to the star are not all exactly zero though; however, they are fairly close, being a few counts up or down from the mean value of zero.

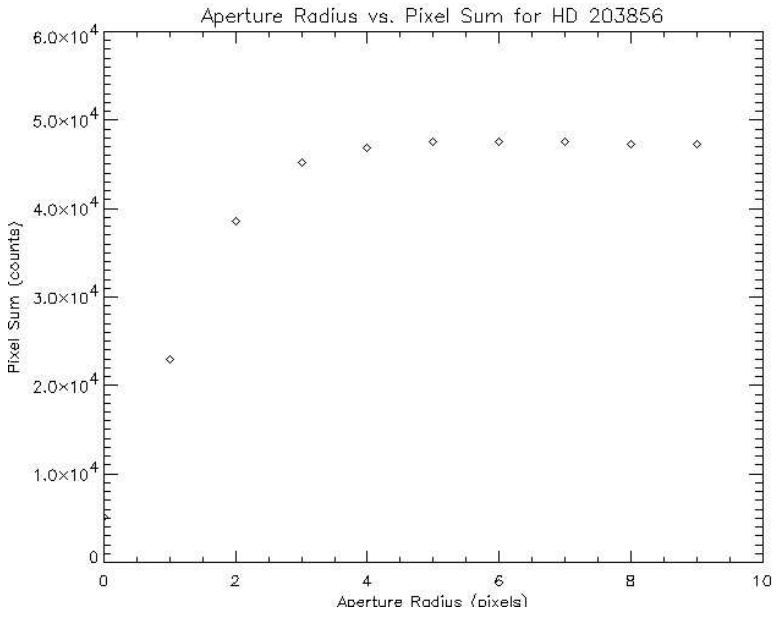

Fig. 7.— Aperture Radius vs. Pixel Sum for HD 203856. Notice the signal fail to increase after a radius of about three pixels for this particular star. The image used had dark current, local sky level, and flatfield subtractions.

4. PHOTOMETRY

Data was extracted for the star HD 3029 in an attempt to determine the apparent magnitude of the star. Nine rastered images, offset by .01 degrees each time in the horizontal and vertical directions, were taken, and the signal was determined for each using the method previously mentioned to collect the total number of counts. By comparing the number of counts received from our star, N^*, with the number of counts received from a star of known magnitude, N_{*known}, the brightness of our star in question can be determined:

$$m^* = m_{*known} + 2.5 \log_{10} \left(\frac{N_{*known}}{t_{*known}} \right) - 2.5 log_{10} \left(\frac{N^*}{t^*} \right)$$

Where t denotes the exposure time, in seconds, of the image. Nine magnitudes were computed for the star, HD 3029, by comparing the counts received from it with the counts received from Gl 105.5, a star of 6.525 magnitude. The results are shown in Figure 8. The mean of the nine magnitudes was computed to be 7.16, with a standard deviation of $\pm .02$. This is very close to the known value for Gl 105.5 of 7.09 magnitudes. The deviation can be attributed to fluctuations in temperature during the imaging process, varying sensitivity of the detector, and changes in weather.

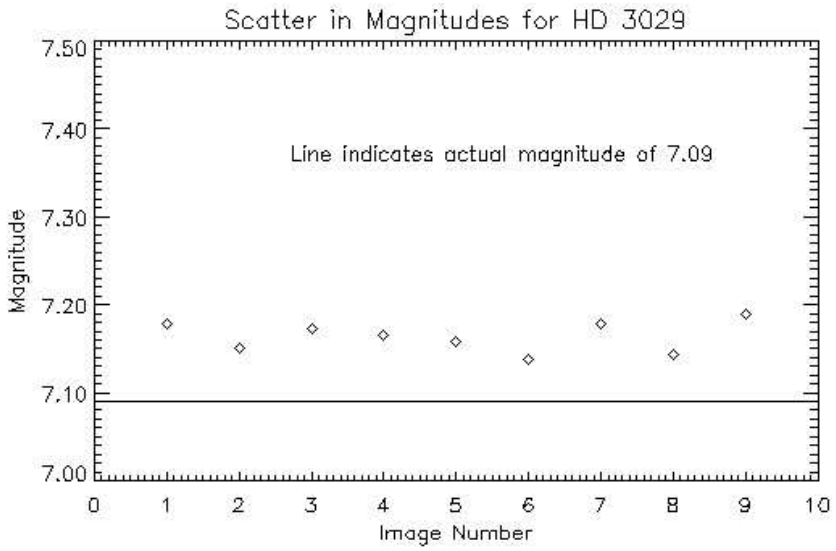

Fig. 8.— Scatter in magnitude for HD 3029. The points indicated the calculated magnitude, and the solid indicates actual (apparent) magnitude.

By measuring the counts for other stars of known magnitude, a conversion factor between the number of photoelectrons per second and the flux of a star can be estimated. The flux of a star can be determined by comparing it to another star of known magnitude:

$$F^* = F_{\nu_0} 10^{-m_\nu / 2.5}$$

This equation is calculated directly from Equation 5 in the Lab 2 handout[5]. The Flux of Vega, a star with 0.0 magnitude, is 636 jansky (10^{-26} W m^{-2}).[6]

Images were taken of HD 201941 (6.625 mag), HD 225023 (6.690 mag), HD 3029 (7.09 mag), and G77-31 (7.840 mag) in an attempt to determine the conversion factor between photoelectrons per second recorded by the detector and the flux from the star. For each star, five separate images were taken; the magnitude for each was computed and converted into flux, and the number of counts for each was converted into photoelectrons. The results are displayed in Figure 9.

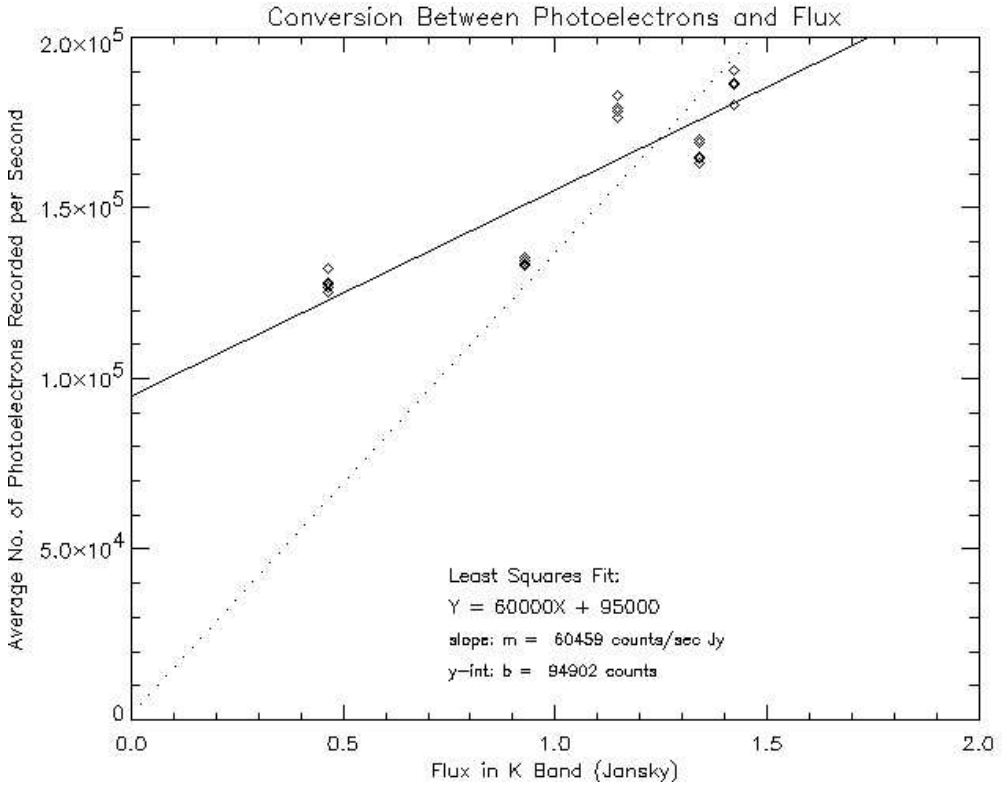

Fig. 9.— Conversion between Flux and Average No. of Photoelectrons Recorded per Second. The solid line displays a least squares fit, and the dotted line displays a least squares fit with the added theoretical point, (0, 0). Five separate exposures were taken for five different stars, for a total of 25 exposures, and the results plotted. Error bars were not include, since they lied within range of the data points (errors were on the order of 70 counts per second.

Unfortunately, the data failed to produce a reasonable least squares fit line (solid line). It would be expected that when no counts are received from a star, the flux would be zero. A theoretical

[5] $m_\nu = -2.5 log_{10}(F_\nu / F_{\nu_0})$

[6] Table 1, Lab 2

point, (0,0), was added to the data in order to better approximate the conversion factor between flux and average number of photoelectrons per second. This yield a conversion factor of 130,000 photoelectrons per jansky.

Ultimately, our goal was to be able to determine what exposure time is necessary to obtain a specific signal-to-noise ratio for a star of a certain magnitude. The signal is the number of counts we receive solely from the star. The noise is composed of the signal, the noise from the background sky, the dark current, and the readout noise. More simply:

$$\frac{S}{N} = \frac{signal}{\sqrt{signal + n_{pix}(\bar{N}_{sky} + \bar{N}_{dark} + \sigma^2_{readout\,noise})}}$$

The signal can be predicted for a star of known magnitude once the conversion factor between flux and photoelectron counts has been determined. Data was gathered for HD 3029, and SAO 054271, and their signal-to-noise ratios were computed at increasing exposure times. Figure 10 displays these results. A rough estimate of this conversion factor, k, was computed using the data on Vega from Table 1, and from Equation 4 in the Lab 2 handout[7]. It was estimated that the factor, k, should be on the order of $10^8 - 10^9$ (J/m^2). This rough guess was used to make a theoretical prediction of the exposure time versus signal-to-noise ratio for a star of known magnitude. As you can see, the theoretical prediction fails to fit the data.

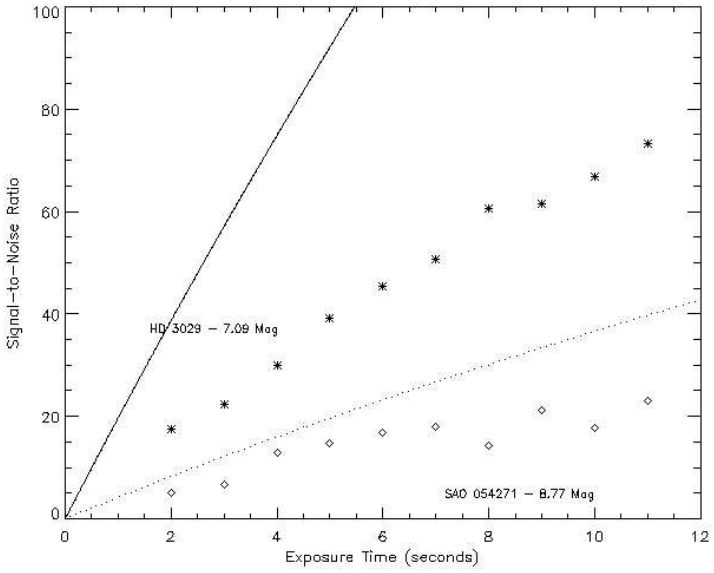

Fig. 10.— Exposure Time vs. Signal-to-Noise Ratio. Plotted points depict measured values. The solid and dotted lines are theoretical predictions for stars with corresponding magnitudes.

[7] $F_\nu = \frac{Nh\nu}{At\Delta\nu\eta_{nu}}$

5. CONCLUSIONS

Ideally, the data would have yielded a conversion factor that would allowed for a more reasonable theoretical plot of signal-to-noise ratios for stars of known magnitudes. Having the ability to predict what exposure time should be used would also us to determine whether or not a signal has been detected from a desired source. It would also help us determine whether or not we made a detection if perhaps we stumbled upon an apparent signal. Various factors might have affected the deviation the conversion factor. Since weather plays a significant role in our photon gathering, it would be ideal to repeat the experiment several more times for several more stars and repeat the examination of the data they yielded.

6. REFERENCES

Taylor, John R. *An Introduction to Error Analysis.* Sausalito: University Science Books, 1997.